The International Journal of Advanced Manufacturing Technology (2023) 126:1789–1797
https://doi.org/10.1007/s00170-023-11124-7

APPLICATION

Replication casting and additive manufacturing for fabrication of cellular aluminum with periodic topology: optimization by CFD simulation

Patricia Fernández-Morales[1] · Lauramaría Echeverrí[2] · Emigdio Mendoza Fandiño[3] · Alejandro Alberto Zuleta Gil[2]

Received: 25 October 2022 / Accepted: 15 February 2023 / Published online: 7 March 2023

Abstract
In this work, processes such as additive digital manufacturing (ADM) and precision casting are presented as alternative methods to manufacture aluminum foams with ordered open-pore morphology. Digital modeling of cellular structures with defined regular patterns was manufactured with ABS and wax and then melted in aluminum A356 alloy by a replication casting process. To guarantee the complete filling of the mold, a simulation by the Flow-3D program was made. This computational tool allowed to determine the temperature values of both melting and the mold temperature. The simulations revealed potential defects in the metal foams to be obtained, which were evidenced by the cast pieces processed after as a validation test. The results show that the casting process carried out supported by a computational fluid dynamics (CFD) simulation allows understanding the effects of the simulated parameter process, optimizing the parameters involved in the infiltration process, and establishing the conditions for obtaining a sound piece of open-cell aluminum foam with truncated octahedron pores shape. The established manufacturing process conditions can be used to produce lattice structures with multifunctional uses such as impact and blast-proof devices, vibration attenuators, or where enhancement of heat transfer could be needed.

Keywords Flow 3D · Investment casting · Additive manufacturing · Metal foams · Periodic topology

1 Introduction

Metallic foams or cellular metals are materials that consist of solid metals with pores distributed throughout their entire volume [1–3]. They can exhibit open or closed porosity and random or ordered pore morphologies, depending on the manufacturing method [4–6]. These porous structures are characterized by having unique combinations of mechanical, physical, and chemical properties, generating great interest in many industrial fields in recent years. In addition, it is a heyday alternative for the formation of sandwich-type structures in combination with materials such as resins reinforced with glass or carbon fibers, taking advantage of its outstanding mechanical properties in vibration absorption as well as the rigidity it possesses thanks to its metallic matrix. [7–9]. Consequently, most reports' properties of the metallic foams can be modulated not only by the matrix material but also by the type of structure it has; their application in varied sectors has certainly led them to be called multifunctional materials [10]. In this way, cellular metals can be used in applications regarding their physical properties like weight reduction, sound absorption, and heat exchange, as well as in applications related to their mechanical properties such as impact energy absorption, load bearing structures, and vibration dampers, among others [11, 12].

Precision casting is one of the most widely used techniques to obtain aluminum foams. The process consists of coating a wax or polymer preform with refractory clay, which is removed by heating while curing the ceramic. Thus, the ceramic remains with a rigid structure, with an internal porous network where the molten metal is poured, thus forming an exact replica of the initial preform [13–17].

✉ Patricia Fernández-Morales
patricia.fernandez@upb.edu.co

[1] Facultad de Ingeniería Industrial, Universidad Pontificia Bolivariana, Circ.1 Nº 70-01, Medellín, Colombia

[2] Grupo de Investigación de Estudios en Diseño - GED, Facultad de Diseño Industrial, Universidad Pontificia Bolivariana, Circ.1 Nº 70-01, Medellín, Colombia

[3] Facultad de Ingeniería Mecánica, Universidad Pontificia Bolivariana, Circ.1 Nº 70-01, Medellín, Colombia

Required pieces with ordered porous structures with control of the size and morphology of the pores, as well as the thickness of the struts have been covered using digital tools such as 3D modeling and additive manufacturing [18–21]. Through its use, it is possible to obtain porous structures with ordered geometry based on polyhedrons such as diamond type, octahedrons, cubes, and hexahedrons, among others. The structures based on the repetition of identical unit cells are known as topologically ordered systems. They have architectural lattice parameters such as connectivity between cells, pore size, and strut thickness [22, 23].

Currently, there are different 3D printing processes such as selective laser sintering (SLS), stereolithography apparatus (SLA), and fused deposition modeling (FDM), each one with its own characteristics but having in common that starts from a 3D digital model obtained by CAD [24].

Many printing techniques have been employed to fabricate polymer components, and although it is possible to find 3D printing of metals that creates parts directly through processes like laser-based, electron-beam-based, arc-based, and ultrasonic welding-based, they are processes considered high cost, both for the equipment and the materials and energy requirements needed [25, 26]. Nevertheless, it is also possible to obtain polymeric models to use as a lost model in precision casting as has been reported by some authors [27–29].

Due to the poor repeatability of the porous structure of the metal foam parts obtained by traditional methods, many of the applications have been limited. Therefore, in many cases, the determination of the adequate process parameters to guarantee the reproducibility of metallic foams with periodic cellular structures is carried out through trial-and-error tests, which causes economic and time losses. For this, required pieces with ordered porous structures with control of the size and morphology of the pores, as well as the thickness of the struts, have been covered using digital tools such as 3D modeling and additive manufacturing, and more interestingly, by combining with the use of computational simulation tools [30, 31].

Modeling and simulation have been used commonly for the study of cellular metals. These types of computational tools have generally been led toward the study of their mechanical [32] or physical properties [33], with few reports related to their use in their manufacturing. Most research are concentrated on closed-pore foams processing, on topics such as bubble decay analysis, bubble expansion, and foam solidification obtained with foaming agent [34–36].

Simulation techniques propose an alternative that allows process optimization, to get casting parts with better quality and fewer defects, also allowing to save additional process costs that could be generated through trial-and-error tests. Programs such as Flow 3D use finite difference or finite volume approximations to numerically solve the fluid and solidification equations leading to preview probable casting defects, relevant support to generate good quality casting parts [37]. This has led to the exploration of new techniques or a combination of existing ones to obtain cellular metals with controlled structures. It is here where simulation and digital manufacturing become extremely valuable tools for optimizing existing processes, particularly those based on the casting process. This work aims to develop a methodology for obtaining aluminum foams with ordered porous structure by combining tools such as additive digital manufacturing, simulation, and precision casting.

2 Materials and Methods

This study was focused on three methodological aspects: (i) preform modeling and manufacturing, (ii) casting simulation process, and (iii) Al foam manufacturing by casting.

2.1 Preform modeling

Rhinoceros3D® and Grasshopper® plugin parametric modeling suite were used to design the porous structures' preforms. To test the capacity of the infiltration process and accuracy of the simulation of preforms with porous structures with greater geometric complexity, two different geometries were designed. These include one with a simple external cubic geometry with spherical pores and the other one with a cubic sample with truncated octahedron pores. The shape and dimensions of the structures and pores were defined in order to work with two representative volumes of basic structures and isotropic pores whose degree of complexity, modeling, and meshing for the simulation did not involve complex morphological variables in order to have a better control simulation and processes variables. The cubic type preforms were designed with dimensions of 48 mm of cube edges, and the cellular structure was made up of spherical pores with a diameter of 7 mm and a cell thickness of 4.5 mm, and others with more complicated structures that comprise truncated octahedron cell shape. The preforms with a truncated octahedron pore structure were designed with dimensions of 50 mm of cube edges, and the cellular structure was constituted by main pores with a diameter of 10 mm, small pores of 2 mm in diameter, and thickness strut of 2 mm. as can be observed in the models in Fig. 1.

By creating points in the three-dimensional space of the software, the unit cells were developed by coordinating each of the vertices of the solid. Multiple repetition structure was given from the establishment of the unit cell formed by polyhedrons.

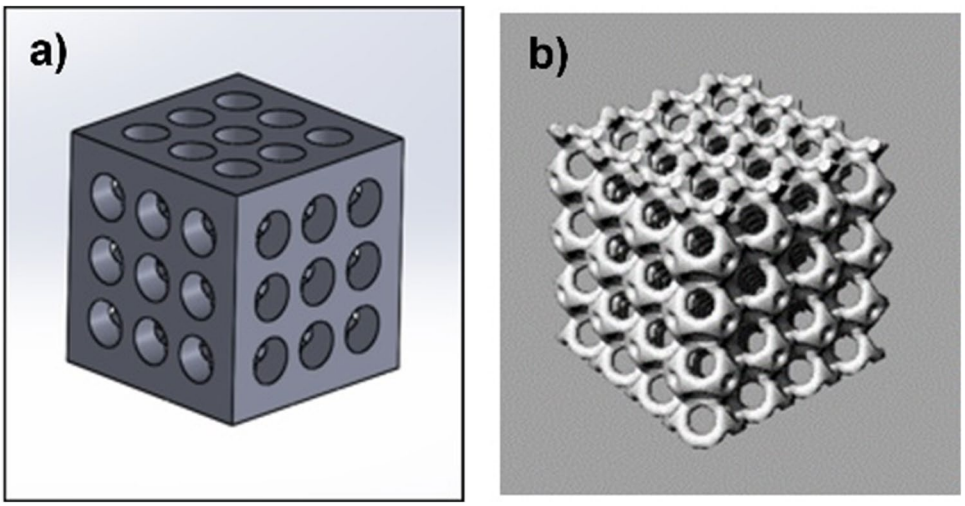

Fig. 1 **a** Foam structure with spherical pores and **b** foam structure with truncated octahedron pores

Table 1 Printing conditions

Infill density (%)	20
Print speed (mm/s)	60
Layer height (mm)	0.15
Extruder temperature (°C)	220

2.1.1 ABS preform manufacturing

After defining the structure, three-dimensional models were created in Rhino® software to generate an STL file to be used in a homemade 3D printer machine [38] using an infill (%) of 20, a feeding rate of 20 mm/s, and a printing temperature of 220 °C. Table 1 indicates the printing conditions.

The preforms in ABS were combined with feeding channels made in wax or ABS. A schematization of the modeling process is shown in Fig. 2.

2.1.2 Casting process simulation

Flow 3D, a computational fluid dynamic (CFD) software, was used to simulate the flow of the melt during the casting as well as the temperature values as a function of time. Flow-3D software discretizes the spatial domain into small cells to form a volume mesh using the finite difference model. The software counts with an internal multi-block meshing system with rectangular elements that allows the level of detail on specified areas of geometry to be increased, then divides the domain into discrete volumes, known as "control volume" approach, to solve the Navier–Stokes [34, 35].

To simulate the pouring of the molds corresponding to the foam structure models, two mesh blocks were used. One for the initial part of the feeder and the second for the rest of the feeder and the model. For the mesh block and the model, a grid with 80,000 cells was adopted, both with a cell size of 0.0024 mm. The casting model setup and mesh block configuration are shown in Fig. 3.

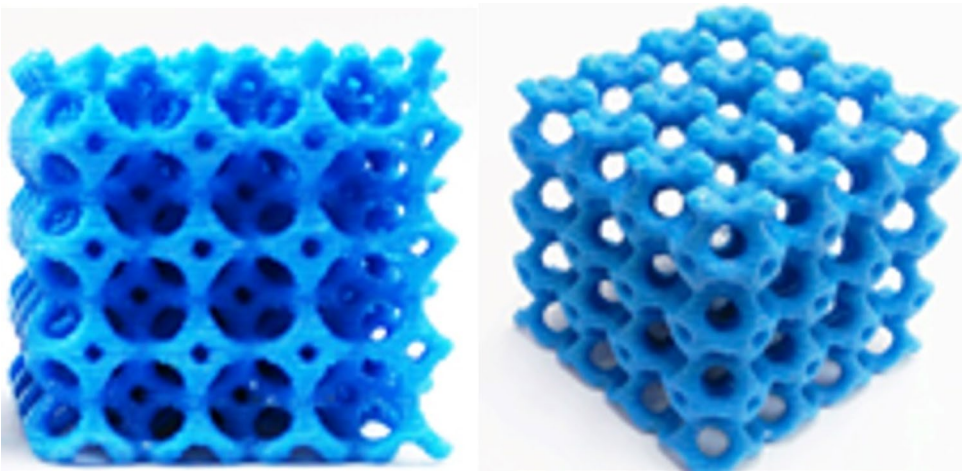

Fig. 2 **a** ABS foam structure with spherical pores and **b** ABS foam structure with truncated octahedron pores

To validate the casting and mold temperature combinations, three mold temperatures at 400 °C, 420 °C, and 440 °C were defined as variables for the simulation, and the metal casting temperatures were settled at 690 °C and 720 °C. A vertical feeding system was defined which would allow the metal to enter the preform from the bottom as shown in Fig. 3.

Material data for both metal and investment materials were required to set up the simulation of the casting process. For the metal, values of viscosity, melting range, the fraction of solid, thermal conductivity, density, and specific heat of aluminum alloy A356 properties were set up [39].

Table 2 Aluminum alloy A356 chemical composition (%w)

Si	Mg	Fe	Cu	Mn	Others
7.24	0.40	0.21	0.014	0.015	Balance

and wax preforms were located singly into a cylindrical steel mold with 125 mm in diameter and 130 mm in height. The ceramic was left to rest for 2 h before being burned at 730 °C. During the burning process, the model was burned allowing the formation of the spaces into the ceramic mold that later was filled by the molten aluminum.

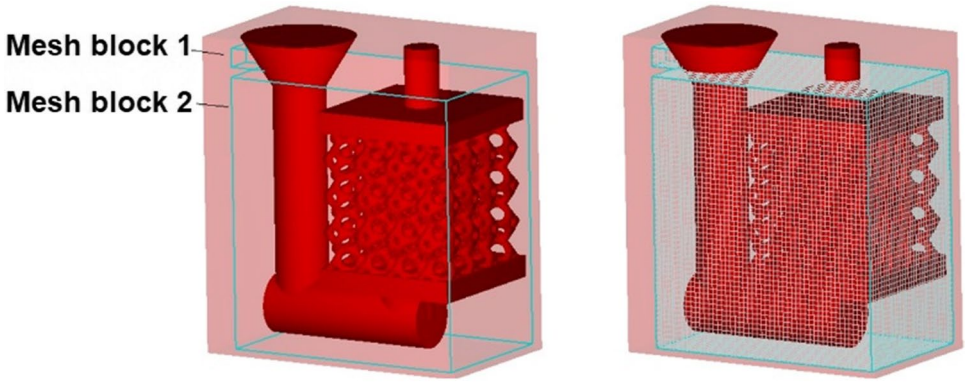

Fig. 3 Casting model setup. **a** Model and **b** mesh block configurations

With regards to the investment material corresponding to the cristobalite, thermal conductivity, density, and specific heat properties were set up. To calibrate the simulation, it is important to mention that preliminary experimental measurements were conducted. In this case, 440 °C was selected for the mold temperature and 720 °C for the casting temperature.

2.1.3 Replication casting process

A KerrCast brand SatinCast 20 coating composed of cristobalite and quartz was used as investment casting. ABS

Aluminum alloy A356 (AlSiMg alloy) was used as the metal matrix. A Shimadzu model OES 5500 optical emission spectrometer was used to determine the chemical composition (%w) as reported in Table 2.

The aluminum foams were obtained by replication casting using a resistance furnace and pouring by gravity. The molten metal was poured into the preheated ceramic mold. The AlSiMg alloy was melted in a graphite crucible.

For each casting process, the ceramic mold was removed by immersion in tap water to break down it and to allow extracting the cast piece. An ultrasonic water cleaner Transsonic TI-H-5 was used to wash away the residual ceramic

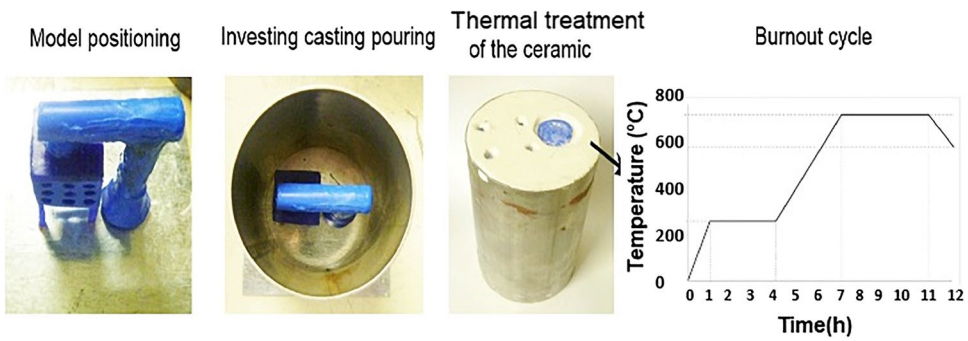

Fig. 4 Preparation of ceramic mold

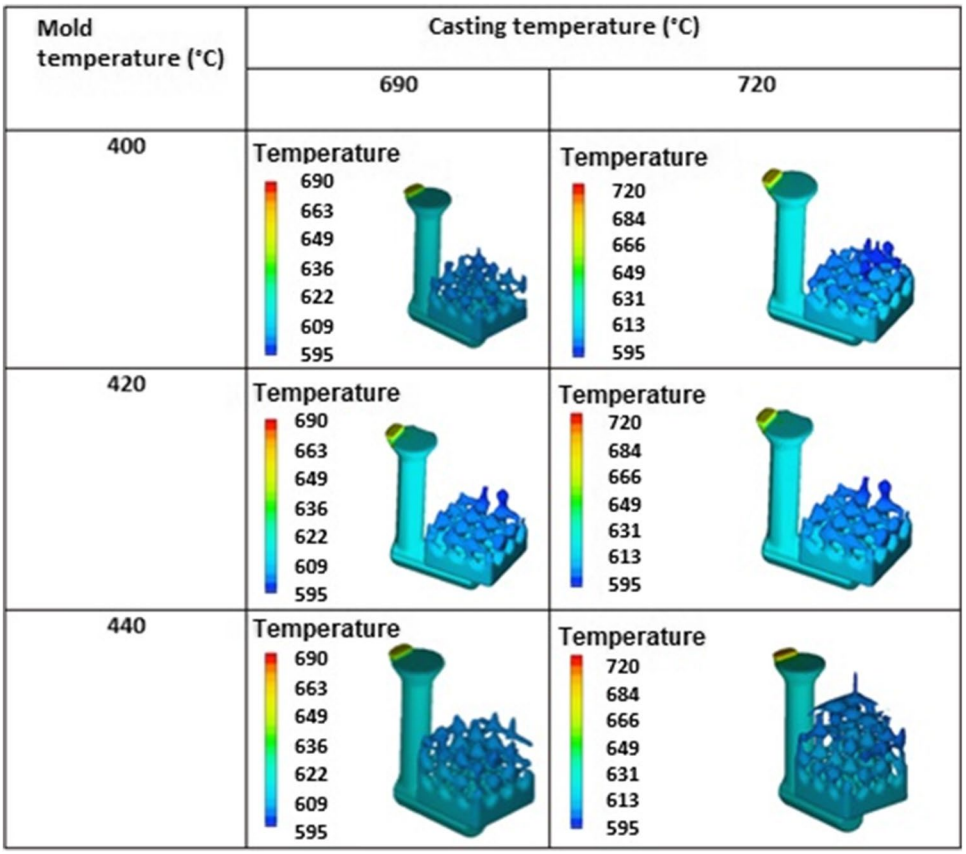

Fig. 5 Simulation software to establish the temperatures of the mold and the casting metal

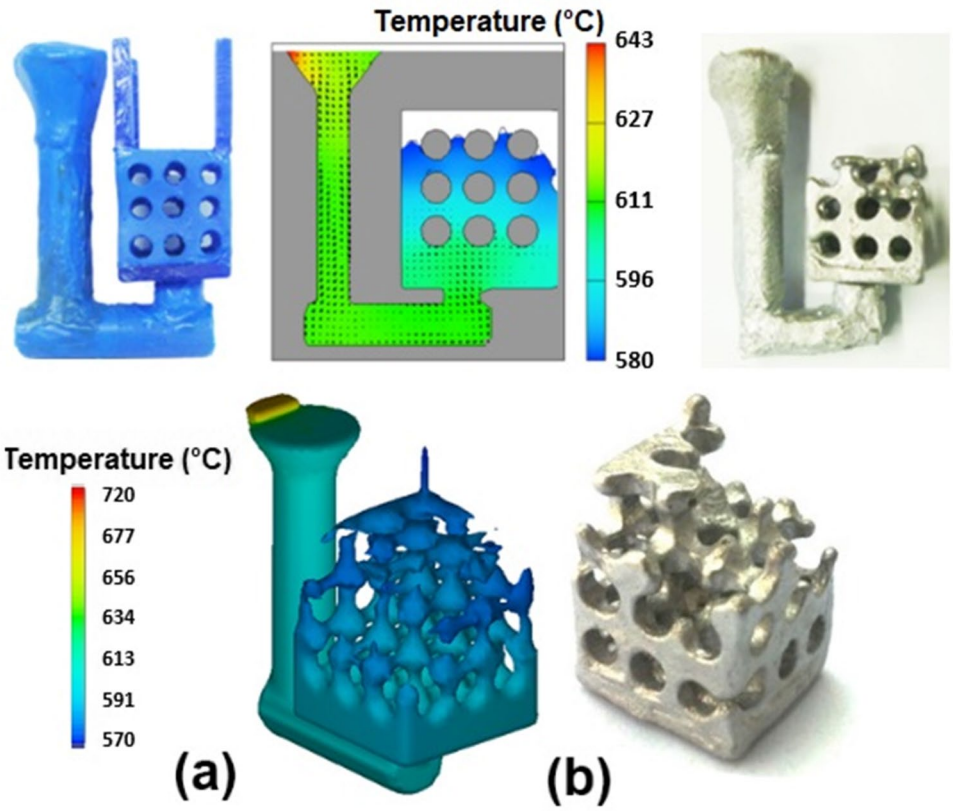

Fig. 6 Validation test of simulation vs casting process. **a** 3D simulation and **b** casting part

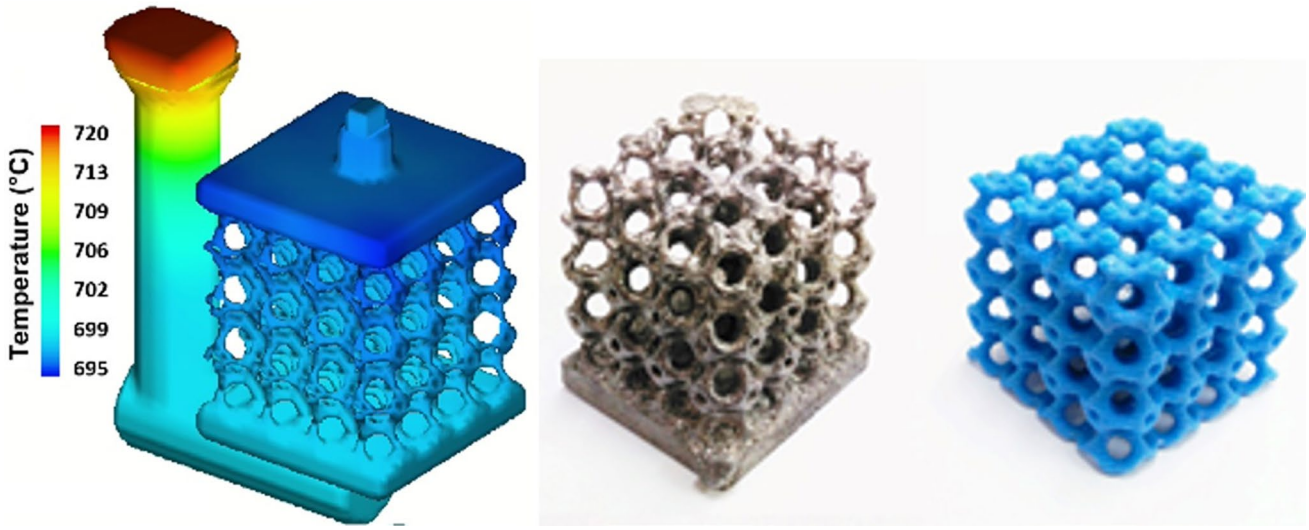

Fig. 7 Obtained foams with truncated octahedron porous morphology

for around 5 min at 25 kHz. The ceramic used allows for obtaining resistant and permeable molds with a high surface finish of the piece, which will be an accurate copy of the initial model. The process is shown in Fig. 4.

3 Results and discussion

When performing the computational simulation of the filling system using Flow 3D, it was found that the filling condition improved as the mold temperature and the casting temperature increased as is observed in Fig. 5.

With the aim to validate the reproducibility of this simulation, it was decided to perform the casting process under the same simulated conditions for one of the combinations of mold and casting temperature: 440 °C and 720 °C, respectively (see Fig. 6).

After this experimentation, it was observed that the cubic shape sample with spherical pores casting obtained was very close to the simulation carried out in Flow 3D as shown in Fig. 6, where, as predicted in the simulation, only around 85% of the casting model was conformed. The experimentation yielded results quite close to those indicated by the simulation; in that way, the simulation parameters were modified, through which it was possible to establish that the optimal temperature conditions for the casting and the mold were 720 °C and 500 °C, respectively.

To test the capacity of the infiltration process and the level of precision of the simulation, preforms with porous structures with greater geometric complexity were used. In this sense, the preform with ordered porosity of truncated octahedron pore morphology was designed. Like the basic structure used for the preliminary tests, in the results obtained for the sample with truncated octahedron porosity and thinner struts, satisfactory casting results were obtained as shown in Fig. 7. This means that a complete filling of the part was obtained throughout its entire structure, showing a very close correspondence to the designed preform modeled in Rhino and obtained by additive manufacturing. It is important to mention that it was found that the material of the wax model and the ABS preform was satisfactorily removed without leaving residues that kept back the filling of the mold, stiffening the refractory structure at the same time.

It was possible to observe that the piece with the least imperfections was the mold specimen with a combination of casting temperature at 720 °C and mold temperature at

Table 3 Correlation between the results for both geometries simulated

Sample structure	Cubic with spherical pores						Cubic with truncated octahedron pores
Dimensions	Cube edges: 48 mm Pore diameter: 7 mm Cell thickness (strut): 4.5 mm						Cube edges: 50 mm Main pore diameter: 10 mm Secondary pore diameter: 2 mm Cell thickness (strut): 2 mm
Mold temp. (°C)	400		420		440		500
Casting temp. (°C)	690	720	690	720	690	720	720
% mold filling	25	32	36	47	70	85%	100%
Casting quality	Incomplete filling						Complete filling

500 °C. That is, a higher temperature of the mold favors the speed with which the casting enters the mold and avoids a large temperature change between the liquid and the solid, reducing damage to the pieces [40]. The results correlation for the two simulated geometries: cubic with spherical pores and cubic with truncated octahedral pores is shown in Table 3. The quality of the part is indicated based on the simulated temperatures and its geometry.

As can be seen, the results of the proposed process are very promising for obtaining quality pieces and high fidelity to the porous structure to be cast. Particularly, this method offers great freedom in design, being possible to generate high porosity with fully reproducible pores, creating homogeneous structures with fully controllable porosity, density, and pore size depending on the preform used, which, depending on the field of application, can be of great value [18, 32]. However, it should also be noted that the process has a high cost per component, since it requires a large number of stages that require a lot of time, high energy expenditure for thermal processes, as well as the cost of the required materials.

As in the present work, some authors have approached techniques such as logistic regression and response surface design to determine the statistical model of the investment casting process to manufacture regular-type aluminum metal foams. The experimental procedure carried out in that report was based on the same investment casting base used in the present work, and although the casting temperature is not reported, there is a coincidence in the temperature of 500 °C used for mold preheating, and as a conclusion, they said that in this process, the geometric characteristics of the foam are important parameters that may have an influence on the successful production [41].

Almost a decade ago, an interesting review concluded about the fascinating trend of integrating additive manufacturing techniques with other manufacturing methods to obtain hybrid structures, among which are scaffolds (open porosity foams) [42]. At that time, it was enunciated as an innovative approach that was in its beginnings; today, it can be said that already it is a reality [43].

4 Conclusions

This study shows the development of a manufacturing process with satisfactory performance for the manufacture of aluminum foams, which combines the 3D printing technique and the replication process optimized by simulating the casting process using Flow-3D software. The combination of programs such as Flow 3D and Rhinoceros as support for the casting process are modeling and simulation tools that facilitate and allow optimization of the process to obtain foams with controlled morphology. This methodology provided great freedom in design, doing possible to generate high porosity fully reproducible in its morphology.

With regard to the casting process, the wax and ABS as preform materials generated by additive manufacturing proved to be suitable for the replication casting process carried out to manufacture aluminum foams with intricate structures.

The results show that the casting process carried out supported by a computational fluid dynamics (CFD) simulation allows understanding the effects of the simulated parameters process optimizing the parameters involved in the infiltration process establishing the conditions for obtaining a sound piece of open-cell aluminum foam with truncated octahedron pores shape. The established manufacturing process conditions can be used to produce lattice structures with multifunctional uses, such as impact and blast-proof devices, vibration attenuators, or where enhancement of heat transfer could be needed.

Even though the process offers the stated advantages, it must be considered that it also presents some disadvantages in addition to those mentioned in the discussions. Among these, it is necessary to validate a greater number of morphologies; the process is limited to a specific type of material and the consideration of the interaction between the mold and the alloy and limitation with the type of alloy.

Author contribution All authors contributed to the study conception and design. Material preparation, data collection, and analysis were performed by L. Echeverri and A. Zuleta. The first draft of the manuscript was written by L. Echeverri, P. Fernández-Morales, and A. Zuleta, and all authors commented on previous versions of the manuscript. All authors read and approved the final manuscript.

Funding Open Access funding provided by Colombia Consortium The authors are grateful to the Centro de Investigación para el Desarrollo y la Innovación (CIDI)—Universidad Pontificia Bolivariana for financial support of this work, through the project Rad. 717C-02–22-18.

Declarations

Competing interests The authors declare no competing interests.

References

1. Ashby MF, Evans AG, Fleck NA, Gibson LJ, Hutchinson JW, Wadley HNG (2000) Making metal foams. Metal foams: a design guide. Butterworth-Heinemann, Woburn, pp 6–23
2. Lázaro J, Solórzano E, Rodríguez-Pérez MA, Kennedy AR (2016) Effect of solidification rate on pore connectivity of aluminium foams and its

consequences on mechanical properties. Mater Sci Eng A 672:236–246. https://doi.org/10.1016/j.msea.2016.07.015
3. Banhart J, Manufacture, (2001) Manufacture, characterisation and application of cellular metals and metal foams. Prog Mater Sci 46:559–632. https://doi.org/10.1016/S0079-6425(00)00002-5
4. Fernández P, Cruz LJ, Coleto J (2008) Manufacturing processes of cellular metals. Part I: Liquid route processes. Rev Metal 44:540–555. https://doi.org/10.3989/revmetalm.0767
5. Fernández P, Cruz LJ, Coleto J (2009) Procesos de fabricación de metales celulares. Parte II: Vía sólida, deposición de metales, otros procesos. Rev Metal 45:124–142. https://doi.org/10.3989/revmetalm.0806
6. Mirzaei-Solhi A, Khalil-Allafi J, Yusefi M, Yazdani M, Mohammadzadeh A (2018) Fabrication of aluminum foams by using $CaCO_3$ foaming agent. Mater Res Express 5:096526. https://doi.org/10.1088/2053-1591/aad88a
7. Cao D, Malakooti S, Kulkarni VN et al (2021) Nanoindentation measurement of core–skin interphase viscoelastic properties in a sandwich glass composite. Mech Time-Depend Mater 25:353–363. https://doi.org/10.1007/s11043-020-09448-y
8. Cao D et al (2021) The effect of resin uptake on the flexural properties of compression molded sandwich composites. Wind Energy. 2022; 25:71–93. https://doi.org/10.1002/we.2661
9. Wang X et al (2021) The interfacial shear strength of carbon nanotube sheet modified carbon fiber composites. In: Silberstein M, Amirkhizi A (eds) Challenges in mechanics of time dependent materials, Volume 2. Conference Proceedings of the Society for Experimental Mechanics Series. Springer, Cham. https://doi.org/10.1007/978-3-030-59542-5_4
10. García-Moreno F (2016) Commercial applications of metal foams: their properties and production. Materials 9:85. https://doi.org/10.3390/ma9020085
11. Atwater MA, Guevara LN, Darling KA, Tschopp MA (2018) Solid state porous metal production: a review of the capabilities, characteristics, and challenges. Adv Eng Mater 20:1–33. https://doi.org/10.1002/adem.201700766
12. Gutiérrez-Vázquez JA, Oñoro J (2008) Espumas de aluminio. Fabricación, propiedades y aplicaciones. Rev Metal 44:457–476. https://doi.org/10.3989/revmetalm.0751
13. Matz AM, Mocker BS, Christian U, Jost N (2014) Microstructural evolution in investment casted open-pore aluminum-based alloy foams. Procedia Materials Science: 8th International Conference on Porous Metals and Metallic Foams, Metfoam 2013:139–144. https://doi.org/10.1016/j.mspro.2014.07.551
14. Matz A, Mocker B, Muller D, Jost N, Eggeler G (2014) Mesostructural design and manufacturing of open-pore metal foams by investment casting. Adv Mater Sci Eng 421729. https://doi.org/10.1155/2014/421729
15. Altug Guler K (2015) Solid mold investment casting –a replication process for open cell foam metal production. Materials Testing 57:795–798. https://doi.org/10.3139/120.110769
16. Sutygina A, Betke U, Hasemann G, Scheffler M (2020) Manufacturing of open-cell metal foams by the sponge replication technique. Symposium on Materials and Joining Technology. IOP Conf Ser: Mater Sci Eng 882 012022. https://doi.org/10.1088/1757-899X/882/1/012022
17. Cingi C, Niini E, Orkas J (2009) Foamed aluminum parts by investment casting. Colloids Surf, A 344:113–117. https://doi.org/10.1016/j.colsurfa.2009.01.006
18. Li Y et al (2018) Additively manufactured biodegradable porous magnesium. Acta Biomater 67:378–392. https://doi.org/10.1016/j.actbio.2017.12.008
19. Li Y et al (2019) Biodegradation-affected fatigue behavior of additively manufactured porous magnesium. Addit Manuf 28:299–311. https://doi.org/10.1016/j.addma.2019.05.013
20. Feng X, Zhang Z, Cui X, Jin G, Zheng W, Liu H (2018) Additive manufactured closed-cell aluminum alloy foams via laser melting deposition process. Mater Lett 233:126–129. https://doi.org/10.1016/j.matlet.2018.08.146
21. Legutko S (2018) Additive techniques of manufacturing functional products from metal materials. IOP Conf Ser Mater Sci Eng 393:012003. https://doi.org/10.1088/1757-899X/393/1/012003
22. Chantarapanich N, Puttawibul P, Sucharitpwatskul S, Jeamwatthanachai P, Inglam S, Sitthiseripratip K (2012) Scaffold library for tissue engineering: a geometric evaluation. Comput Math Methods Med 2012:407805. https://doi.org/10.1155/2012/407805
23. Wenninger MJ (2015) Polyhedron models. Cambridge University Press. https://doi.org/10.1017/CBO9780511569746
24. Stansbury JW, Idacavage MJ (2016) 3D printing with polymers: challenges among expanding options and opportunities. Dent Mater 32:54–64. https://doi.org/10.1016/j.dental.2015.09.018
25. Das S, Bourell DL, Babu SS (2016) Metallic Materials For 3D Printing. MRS Bull 41:729–741. https://doi.org/10.1557/mrs.2016.217
26. Wei Ch, Li L, Zhang X, Chueh Y-H (2018) 3D printing of multiple metallic materials via modified selective laser melting. CIRP Ann 67:245–248. https://doi.org/10.1016/j.cirp.2018.04.096
27. Costanza G, Tata ME, Trillicoso G (2021) Al foams manufactured by PLA replication and sacrifice. Int J Lightweight Mater Manufac 4:62–66. https://doi.org/10.1016/j.ijlmm.2020.07.001
28. Pinto P, Peixinho N, Soares D, Silva F (2015) Process development for manufacturing of cellular structures with controlled geometry and properties. Mat Res 18:274–282. https://doi.org/10.1590/1516-1439.286614
29. Cheah CM, Chua CK, Lee CW, Feng C, Totong K (2005) Rapid prototyping and tooling techniques: a review of applications for rapid investment casting. Int J Adv Manuf Technol 25:308–320. https://doi.org/10.1007/s00170-003-1840-6
30. Heiss T, Klotz UE, Tiberto D (2015) Platinum investment casting, part I: simulation and experimental study of the casting process. Johnson Matthey Technol Rev 59:95–108. https://doi.org/10.1595/205651315x687399
31. Grande MA, Porta L, Tiberto D (2007) Computer simulation of the investment casting process: widening of the filling step. The Santa Fe Symposium Jewelry Manufacturing Technology 1-18:53658215
32. Kader MA, Islam MA, Hazell PJ, Escobedo JP, Saadatfar M, Brown AD, Appleby-Thomas GJ (2016) Modelling and characterization of cell collapse in aluminium foams during dynamic loading. Int J Impact Eng 96:78–88. https://doi.org/10.1016/j.ijimpeng.2016.05.020
33. Pulvirenti B, Celli M, Barletta A (2020) Flow and convection in metal foams: a survey and new CFD results. Fluids 5:155. https://doi.org/10.3390/fluids5030155
34. Diop M, Hao H, Dong H-W, Zhang X-G, Yao S, Jin J-Z (2011) Modelling of solidification process of aluminium foams using lattice Boltzmann method. Int J Cast Met Res 24:158–162. https://doi.org/10.1179/136404611X13001912813861
35. Hao H, Diop M, Yao S, Zhang X-G (2010) Numerical simulation of bubbles expansion and solidification of metal foams. Mater Sci Forum 654–656:1549–1552. https://doi.org/10.4028/www.scientific.net/MSF.654-656.1549
36. Barzegari M, Bayani H, Mirbagheri SMH, Shetabivash Ha (2019) Multiphase aluminum A356 foam formation process simulation using lattice Boltzmann method. J Market Res 8:1258–1266. https://doi.org/10.1016/j.jmrt.2018.03.010
37. Barkhudarov MR, Hirt CW (1995) Casting simulation: mold filling and solidification-benchmark calculations using flow-3D. In Proceedings of the Ninth International Conference on Modeling of Casting, Welding and Advanced Solidification Processes. https://www.flow3d.com/wp-content/uploads/2014/08/Casting-Simulation-Mold-Filling-and-Solidification-Benchmark-Calculations-Using-FLOW-3D.pdf
38. Dizon JRC, Espera AH, Chen Q, Advincula RC (2018) Mechanical characterization of 3D-printed polymers. Addit Manuf 20:44–67. https://doi.org/10.1016/j.addma.2017.12.002
39. Matweb (1996) www.matweb.com

40. Staff FMT, & Foundry Management and Technology (2015) Why infrared heating stands apart for preheating sand molds. Retrieved August 2, 2017, from http://www.foundrymag.com/moldscores/hot-idea-mold-preheating-and-more.
41. Anglani A, Pacella M (2018) Logistic regression and response surface design for statistical modeling of investment casting process in metal foam production. Procedia CIRP 67:504–509
42. Giannitelli SM, Accoto D, Trombetta M, Rainer A (2014) Current trends in the design of scaffolds for computer-aided tissue engineering. Acta Biomater 10:580–594
43. Dumas M, Terriault P, Brailovski V (2017) Modelling and characterization of a porosity graded lattice structure for additively manufactured biomaterials. Mater Des 121:383–392